

Low Cost Vision-Based Multi-Lane Road Marker Recognition and Vehicle Pose Estimation

Sofyan Tan and Rudy Susanto, *Members, IEEE*

Abstract— Implementation of vision-based lane detection system in vehicle usually needs high detection rate for reliability. However the implementation can be limited by the calculation power available in the vehicle. This paper reports an improvement of our previous approach while keeping the processing power low. The algorithm proposed in this paper avoid heavy pixel-by-pixel image processing of the captured image, it works mostly on the detected line segments instead of the image. The proposed algorithm is also more global, capable in recognizing multiple lane markers and estimating the position of the vehicle on a multi-lane road. The algorithm is evaluated using miniature road and miniature vehicle for various poses. The recognition rate and the estimation accuracy are shown to be much higher with only 1% failure rate compared to the previous approach in [12] or [13].

Index Terms—Hough transform, inverse perspective mapping, multi-lane recognition, vehicle pose estimation.

http://www.ieee.org/organizations/pubs/ani_prod/keywrd98.txt

I. INTRODUCTION

The future of automobiles is predicted to include a lot of automations [1]. In fact autonomous cars are under researched and tested in many countries by many institutions [2]-[3]. Some of the purposes of having autonomous car are to reduce traffic accidents caused by human error, to increase comfort, and to increase the capacity of the road. One important information for autonomous car is the pose of the

vehicle relative to the road lane, which include the lateral position of the vehicle and the orientation of the vehicle relative to the lane. Many of the related research road for lane recognition system involve the Hough transform [4]-[8], Gabor Filter [5], [9], geometrical model [5], Fuzzy reasoning [8], or color features [10]. Some also use inverse or warp perspective mapping [6], [9], [11] to remove skewing caused by projection of 3D world to the 2D image in the camera.

Most of these approaches require relatively high calculation cost that can limit their implementation in power limited and environment friendly vehicles. Our objective in this research is to develop a low cost algorithm for lane markers recognition and vehicle pose estimation on a multi-lane road.

In this research we extend our low cost single-lane recognition algorithm in [12] and [13] to cover multiple lanes and to improve the lane recognition rate and estimation accuracy while maintaining the low cost nature of our algorithm. Instead of working directly on the image to recognize the lane markers, the algorithm uses the probabilistic Hough transform [14], to detect the lines in the source image. From this point forward the entire multi-lane recognition algorithm works only on the line's coordinates which are much less than the number of pixel in the original image.

II. IMAGE PRE-PROCESSING AND LINE DETECTION

Assuming that the camera's optical axis is parallel to the flat road, the vanishing point of the lane will be at the center row of the captured image. Therefore the information above the center row of the image can be neglected, and further image processing only applies to the lower half of the image to improve calculation speed.

Canny edge detection is used to obtain the binary edge information from the captured gray image. The binary edge contains less number of non-zero pixels compared to the gray image. The lesser the pixels, the lesser the calculation cost to do Hough transformation of the edge image in order to detect lines in the image.

Since the lane is assumed straight at up to an adequate distance, then most part of the lane markings will show up as straight lines. Lane markings at further distance from the camera will be projected to smaller number of pixels in the image. Hence Hough transform of the edge image will mainly detect lines near to the camera.

Manuscript received October 2, 2015. This work was supported by research grant from the Indonesian Ministry of Technology Research and Higher Education.

Sofyan Tan is with the Automotive and Robotics Engineering, BINUS ASO School of Engineering, Bina Nusantara University, Alam Sutera, Serpong, Indonesia (e-mail: sofyan@binus.edu). He received his B.S. degree in Computer Engineering from Bina Nusantara University, Jakarta, Indonesia, in 2002, and his M.Eng. degree in Electronics Engineering from the University of Tokyo, Tokyo, Japan, in 2008.

Rudy Susanto is with the Computer Engineering Department, Bina Nusantara University, Jakarta, Indonesia, (phone: +6221-53696930; e-mail lierudys@gmail.com). He received his B.S. degree in Computer Engineering and M.S. degree in Computer Science both from Bina Nusantara University.

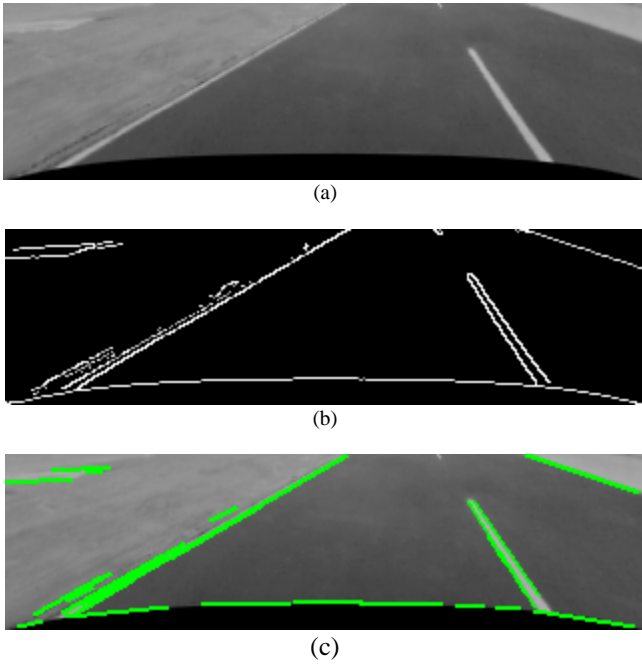


Fig. 1. Example of the line detection process, where (a) is the grayscale image, (b) is the edge binary image, and (c) shows the detected lines in bold green.

Fig. 1 shows an example of the implemented line detection process, where only the lower half of the image from the camera is used. Canny edge detection operator is applied to mark edges in the image, and then the progressive probabilistic Hough transform detect line segments from the edge binary image shown as bold green lines in the figure. Note that the black area at the bottom of the image is a result of undistorted process to remove barrel distortion caused by the imperfection of the camera's wide angle lens.

III. THE INVERSE PERSPECTIVE MAPPING

To correct the perspective view of the scene, we apply inverse perspective mapping (IPM). These mappings yields bird's view estimate of the scene where lane markings are parallel to each other. These methods usually perform mapping of the whole image as in [6], [9], [11].

However to reduce computational cost, we reduce the mapping of the whole image into the mapping of the line segments using IPM. The mapping of each line segment involves the mapping of the starting and ending coordinate of each line segment. Assuming the pinhole camera model, we can find the road plane coordinate (X, Z) from the image coordinate (x, y) of each the starting or ending of the line segment according to equation (1).

$$Z = \frac{F_y Y}{y - O_y} \text{ and } X = \frac{Z(x - O_x)}{F_x}, \quad (1)$$

where (O_x, O_y) is the image coordinate of the principal point. F_x and F_y are the focal length of the camera measured in pixels according to the pixel pitch in the column and row direction respectively. The other intrinsic parameters of the camera are

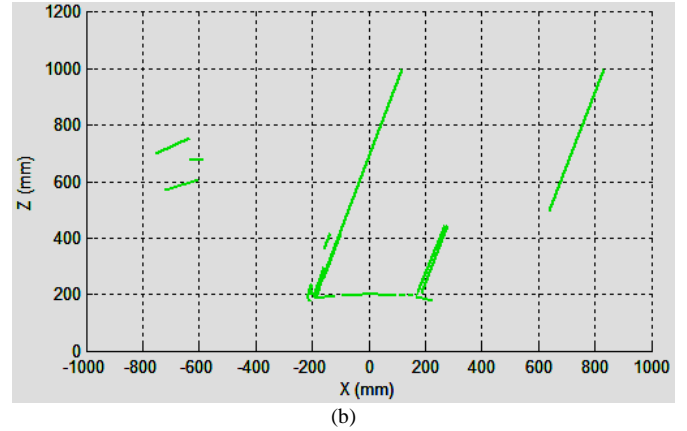
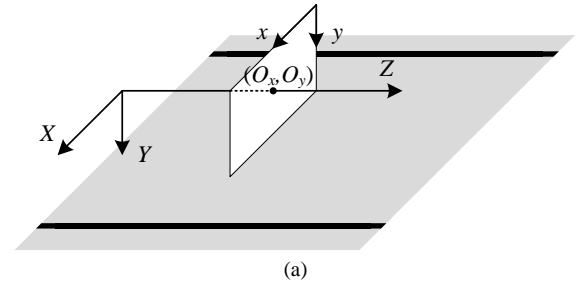


Fig. 2. (a) Coordinate system of the image plane and (b) the example of the resulting inverse perspective mapping of the line segments in road plane coordinate (bird's view).

assumed to be zero. Note that the intrinsic parameters of the camera can be measured with precision by doing camera calibration.

The coordinate system of the road plane and the image plane is depicted in Fig. 2(a). In our case the height of the camera from the road Y is assumed to be constant. The optical axis of the camera is assumed parallel to the lane direction and the optical center is directly above the center of the lane.

The resulting line segments after the IPM of the line segments in Fig. 1(c) are shown in fig 2(b). The line segments representative of the lane markings in road plane coordinate will be parallel to each other, which simplify the lane recognition. However because the extrinsic parameters, which are the height, pitch, and roll of the camera cannot be kept perfect all the time during operation, some mapping error are expected.

IV. RECOGNIZING THE LANE MARKERS AND ESTIMATING VEHICLE ORIENTATION

The algorithm proposed here to recognize the lane markers is more global compared to the one in [12] and [13]. Instead of searching for a pair of longest parallel line segments with suitable distance, we search for one set of parallel line segments, which distances are integer multiple of the known road wide, that contains the maximum number of line segments. There can be multiple sets of parallel line segments with suitable distances, but it takes the one with the maximum number of members to reduce the probability of false positive. Estimation accuracy of the vehicle orientation on the road

plane can also be increased by averaging the angles of many line segments in the set. The vehicle orientation θ_e is calculated according to the equation (2), where θ_{en} is the angle of each line segment.

$$\theta_e = \frac{1}{N} \sum_{n=1}^N \theta_{en} \quad (2)$$

The vehicle angle is zero when the vehicle is heading straight along the road's direction, negative when the vehicle is heading to the left, and positive when the vehicle is heading to the right. The details on the calculation on θ_{en} can be seen in [12] and [13]. After obtaining the vehicle orientation, all the chosen line segments can be rotated by $-\theta_e$ to simplify the lateral position estimation.

The rotated line segments are further grouped according to their lateral distances in order to estimate the location of each individual lane marker. Fig. 3 shows one example of the set of parallel line segments chosen from the detected lines in Fig. 2(b). The grouping of line segments in the chosen set in Fig. 3 will give three different groups of line segments for the leftmost, center, and rightmost lane markers. The average lateral position of the line segments in each group will become the lateral position of a lane marker.

V. PROBABILITY OF DASHED AND SOLID LANE MARKERS

In order to improve the accuracy of the lane markers recognition, the algorithm also identifies the type of lane marker by calculating the probability of solid lane marker and the probability of dashed lane marker for each group of line segments. Each dashed lane marker is shorter in length compared to solid lane marker and there can be more than one dashed lane marker in a line. Therefore the algorithm should calculate the length of each marker in a group by calculating the combined length of overlapping line segments, and it should also calculate the distance to the next marker in a group, when available.

However the actual dashed or solid lane markers on the road can be easily damaged by usage and weather, and they can also be easily blocked from the view of the camera. Therefore calculating the probability of detecting a line of dashed lane markers and the probability of detecting a solid lane marker are more appropriate in this situation.

The probabilities of detecting a solid lane marker in a group of line segments is calculated based on the combined length of the overlapping line segments in a group. The probability P_{solid} is calculated using modified Gaussian function (3), where any combined length l that is equal or longer than a maximum length c_{solid} will have a probability of one. When there are more than one overlapping line segments in a group then the probabilities will be summed.

$$P_{solid}(l) = \begin{cases} 1, & \text{if } l > c_{solid}; \\ \exp\left(-\frac{(l - c_{solid})^2}{2\sigma_{solid}^2}\right) & \text{otherwise.} \end{cases} \quad (3)$$

By knowing the full width at half maximum (FWHM) of the

half Gaussian function, $FWHM = 2\sigma\sqrt{2\ln 2}$, we can calculate the standard deviation σ_{solid} so that the probability is half or lower when the combined length is equal or lower than a minimum length m_{solid} of solid lane marker respectively using equation (4).

$$\sigma_{solid} = \frac{(c_{solid} - m_{solid})}{\sqrt{2\ln 2}} \quad (4)$$

The probability of detecting one or more dashed lane marker(s) in a group is calculated based on the combined length of overlapping line segments and the separation between the overlapping line segments in a group. The probability P_{dashed} is calculated using Gaussian functions (5), where the function is at maximum when the combined lengths l_k are equal with an ideal length c_{dashed} and the separation d between the overlapping line segments in a group is equal with an ideal separation c_{dist} , where $k = 1, 2$ is the index of the overlapping line segments, assuming a maximum of two overlapping line segments in a group.

$$P_{dashed}(l) = \frac{1}{3} \exp\left(-\frac{(l_1 - c_{dashed})^2}{2\sigma_{dashed}^2}\right) + \frac{1}{3} \exp\left(-\frac{(d - c_{dist})^2}{2\sigma_{dist}^2}\right) + \frac{1}{3} \exp\left(-\frac{(l_2 - c_{dashed})^2}{2\sigma_{dashed}^2}\right) \quad (5)$$

Similarly, the standard deviation σ_{dashed} and σ_{dist} can be calculated so that the probability is half when the difference between the combined length and the ideal length is equal a maximum length difference δ_{dashed} (6), and the difference between the separation and the ideal separation is equal a maximum separation difference δ_{dist} (6) respectively.

$$\sigma_{dashed} = \frac{\delta_{dashed}}{\sqrt{2\ln 2}} \quad \text{and} \quad \sigma_{dist} = \frac{\delta_{dist}}{\sqrt{2\ln 2}} \quad (6)$$

VI. ESTIMATION OF THE LATERAL POSITION

The lateral position of a vehicle on a multi-lane road depends on the amount of lane markers recognized from the captured image. In the experiment we are assuming that there are two lanes on the road and that the center lane marker are dashed. With that assumption, the estimation of the lateral position includes the estimation of left and right lane based on the recognized lane markers.

The number of lane detected can be calculated from the lateral distance between the leftmost and the rightmost group of lane markers. A lateral distance that is similar to the lane's width means that one lanes has been detected, while a lateral distance that is similar to twice the lane's width means that two lanes has been detected. The algorithm cannot recognize the lane when only one group of lane markers is detected.

TABLE I
ESTIMATION CALCULATION FOR ALL POSSIBLE CONDITIONS

Conditions	Lateral Position Estimation
1. One lane is detected:	
1.1. Left is solid, right is dashed	$L_e = -(D_{left} + D_{right}) / 2$
1.2. Left is dashed, right is solid	$L_e = -(D_{left} + D_{right}) / 2 - W$
2. Two lanes are detected:	
2.1. There are two groups of lane markers	$D_{middle} = (D_{left} + D_{right}) / 2$ $L_e = -(D_{left} + D_{middle}) / 2$
2.2. There are three groups of lane markers	$L_e = -(D_{left} + D_{middle}) / 2$

The proposed algorithm searches for all possible positions of the lane markers in the two-lane road and choose one condition that gives the highest probability. In total there are only two possible conditions to check when there is one lane detected, and only two possible conditions when there are two lanes detected.

When the position of lane markers have been estimated then the lateral position of the vehicle can be estimated based on the position of the lane markers. The details of the calculation to estimate lateral position can be seen in Table 1 for all possible conditions. For simplicity the lateral position L_e is always calculated from the center of left lane, even though the vehicle is at the right lane. The lateral position relative to the center of the right lane is simply $L_e -$ the lane's width W .

VII. EXPERIMENT RESULTS AND ANALYSIS

The experiment is using miniature multi-lane road and miniature vehicle that are 1/10 the size of the actual road and vehicle, as depicted in Fig 3(a) and (b). The miniature road is painted on a board (1.6 m \times 0.72 m) with lane's width of 355 mm. The miniature vehicle was a remote controlled toy car with an attached wide angle (120° view angle) webcam® that is connected to the camera on the vehicle in order to do the experiment.

To evaluate the accuracy of the algorithm to recognize the lane markings and to estimate the vehicle's pose, we put the vehicle in 4 different lateral positions, as shown in Fig 3(c). All the lateral positions are relative to the center of the left lane, where positive positions are to the right of the center of the left lane. At each lateral position the vehicle's orientation is varied into 4 different angles from 0 to -30 degrees. Negative orientation means that the vehicle diverges to the left of the road's direction. Positive orientations are neglected because of the symmetrical nature of the problem.

Out of the 16 poses only at 0° and lateral position 355mm that the system has 99% recognition rate, while others can perfectly recognize the lane markers. Failure occurs when the algorithm fails to detect at least two correct lane markers or at least one correct lane. These failures are generally caused by the lack of lane marker captured by the camera because of large orientation angle, or caused by disturbance in the environment that resembles the lane markers.

The accuracy of the pose estimation is shown in Fig. 4 for

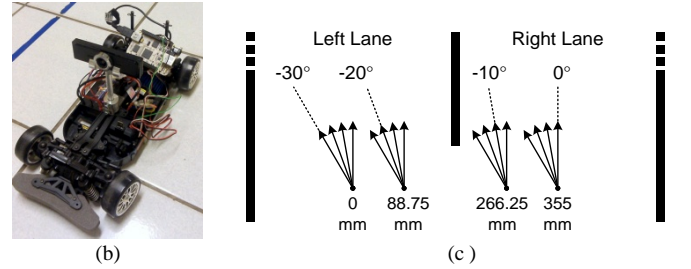
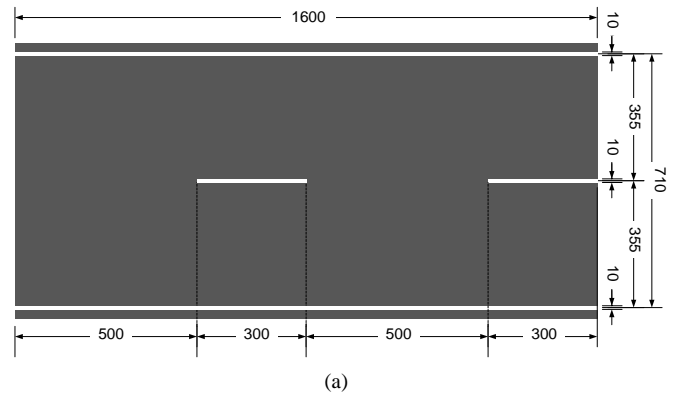


Fig. 3. (a) The miniature road lane, (b) the miniature vehicle, and (c) the 16 poses of the vehicle, with 4 different lateral positions (relative to the center of the left lane) and 4 different orientations.

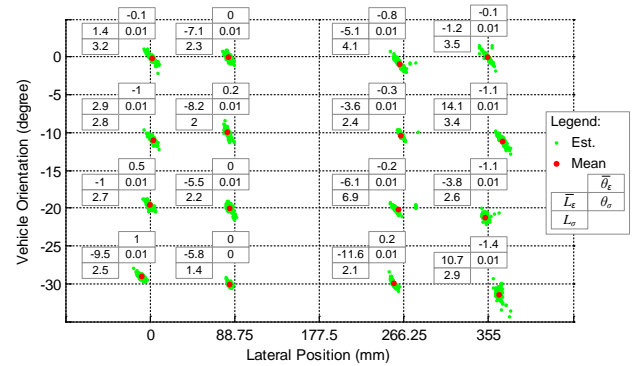


Fig. 4. Pose estimation results with mean lateral error \bar{L}_e , mean orientation error $\bar{\theta}_e$, lateral standard deviation L_σ , and orientation standard deviation θ_σ .

all 16 poses that are tested in the experiment. The maximum mean lateral error is 14.1 mm, which is 4% of the lane's width. In many poses the mean lateral error is less than 10 mm. The lateral position estimation is more prone to error because it is sensitive to the roll of the camera about its optical axis, which is caused by the overly soft suspension of the miniature vehicle. The maximum lateral standard deviation is only 6.9 mm. This quite good considering that the lane marker has a width of 10 mm and the line can be detected in either side of the lane marker.

Vehicle orientation estimation results is highly accurate for many applications, where the maximum mean estimation error is only 1.4°, and the standard deviations are only 0.01° or lower.

The worst case average lateral estimation error is 14 mm which occur at the lateral position of 355 mm and vehicle

orientation of -10^0 . Although it is relatively high (4% of the lane's width), the standard deviation at that particular pose is only 3.4 mm (from fig. 4) which is much less than the average lateral standard deviation for all poses in [13] (which is 8.57 mm) as shown in Table II. The average lateral standard deviation across all poses is even smaller at 2.93 mm. This result shows that the error is relatively constant, most probably caused by inaccuracy during the experiment setup, not because of the inaccuracy of the proposed algorithm. The standard deviations of the vehicle orientation estimations are also very small at 0.01^0 , which is much smaller than that achieved in [12] and [13].

VIII. CONCLUSIONS

We have presented an algorithm to recognize lane markers in a multi-lane road, and to estimate vehicle lateral position and its orientation. The algorithm do more calculation compared to the one in [12] and [13], but all the additional calculation are only performed on the line segment coordinates, which is insignificant in number compared to the number of pixels in the image captured by the camera. The proposed algorithm can be generalized for one, two, or more lanes, assuming that the actual number of lane and the lane dimensions are known.

In overall the recognition rates are much better than the results in [12] or [13] because the current algorithm chooses the best set of line segments instead of only the best pair of line segments. It is also because we have more lane markers to be found which reduce the probability of not finding enough lane markers. The pose estimation accuracy is also better than [13] even when the vehicle orientation is at its extreme angles as seen in table II.

In the future, the evaluations of this new approach on one or more types of embedded computers are attractive in order to see the real-time performance of the algorithm. Development of the lateral control algorithm using this approach as the feedback is also desired for future research.

TABLE II
COMPARISON OF EXPERIMENT RESULT BETWEEN ALGORITHM IN THE
EXPERIMENT WITH [12] AND [13]

Parameter	Current	[13]	[12]
Operable Lateral position	-355 to 355 mm	-200 to 200 mm	-50 to 50 mm
Operable Vehicle orientation	-30^0 to 30^0	-25^0 to 25^0	-10^0 to 10^0
Average Lateral Standard Deviations ($L\sigma$)	2.93 mm	8.57 mm	5.1 mm
Average Orientation Standard Deviations ($\theta\sigma$)	0.01^0	0.800^0	0.303^0
Lowest Recognition rate	99% in 0^0	90% in -20^0 and 70% in -25^0	78% in -10^0 and -5^0

REFERENCES

- [1] L. Guzzella, "The Automobile of the Future – Option for Efficient Individual Mobility," IEEE Control Applications, (CCA) & Intelligent Control, (ISIC). Plenary talk, 2009.
- [2] Philip E. Ross, "Robot, you can drive my car," in IEEE Spectrum, 2014, pp. 60-90 (Vol. 51, Issue. 6).
- [3] G. Obinata, T. Suzuki, and T. Wada, "Tutorial I: Car robotics — Self-driving cars and human factor," in SICE Annual Conference (SICE) 2012, 2012, pp. xiv.
- [4] M. Caner Kurtul, "Road Lane and Traffic Sign Detection & Tracking for Autonomous Urban Driving," Bogazici University, Istanbul, Master Thesis 2010.
- [5] Shengyan Zhou et al., "A novel lane detection based on geometrical model and Gabor filter," in IEEE Intelligent Vehicle Symposium, San Diego, CA, 2010, pp. 59 - 64.
- [6] Fangfang Xu, Bo Wang, Zhiqiang Zhou, and Zhihui Zheng, "Real-time lane detection for intelligent vehicles based on monocular vision," in 31st Chinese Control Conference, Hefei, 2012, pp. 7332 - 7337.
- [7] Abdulhakam.AM. Assidiq, Othman O. Khalifa, Md. Rafiqul Islam, and Sheroz Khan, "Real Time Lane Detection for Autonomous Vehicles," in International Conference on Computer and Communication Engineering, Kuala Lumpur, 2008, pp. 82-88.
- [8] Ping Kuang, Qingxin Zhu, and Guochan Liu, "Real-time road lane recognition using fuzzy reasoning for AGV vision system," in International Conference on Communications, Circuits and Systems, June, 2004, pp. 989-993 Vol.2.
- [9] F. Coşkun, O. Tunçer, M.E. Karşilgil, and L. Güvenç, "Real time lane detection and tracking system evaluated in a hardware-in-the-loop simulator," in International IEEE Conference on Intelligent Transportation Systems, Funchal, 2010, pp. 1336 - 1343.
- [10] Ping Kuang, Qinxing Zhu, and Xudong Chen, "A Road Lane Recognition Algorithm Based on Color Features in AGV Vision Systems," in International Conference on Communications, Circuits and Systems, Guilin, 2006, pp. 475 - 479 (Vol. 1).
- [11] A.M. Muad, A. Hussain, S.A. Samad, M.M. Mustafa, and B.Y. Majlis, "Implementation of Inverse Perspective Mapping Algorithm for the Development of an Automatic Lane Tracking System," in IEEE Region 10 Conference TENCON 2004, 2004, pp. 207 - 210 (Vol. 1).
- [12] S. Tan, and J. Mae, "Real Time Lane Recognition and Position Estimation for Small Vehicle," Internetworking Indonesia Journal, 2013, pp. 3 – 8 (Vol. 5, No. 2 B).
- [13] S. Tan, Agnes, and J. Mae, "Low Cost Vision-Based Real-Time Lane Recognition and Lateral Pose Estimation," in IEEE International Conference on Computational Intelligent and Cybernetics, 2013, pp. 151 - 154.
- [14] J. Matas, C. Galambos, and J.V. Kittler, "Robust Detection of Lines Using the Progressive Probabilistic Hough Transform," Computer Vision and Image Understanding, vol. 78, no. 1, pp. 119-137, April 2000.